AJS

Algerian Journal of Sciences
Volume 2 – Issue 1 – PP. 37 – 49

Natural Oxidation of Polyethylene in semi-aride climate: Insights into Structural and Chemical Changes

Souad Djellali[1,2*], Yasmine Abdelouahed[1], Tahar Sadoun[3], Yves Grohens[4]
[1]Department of Chemistry, Faculty of Sciences, University Setif 1 Ferhat Abbas, 19000, Setif, Algeria

[2]Laboratory of Physical Chemistry of High Polymers, University Setif 1 Ferhat Abbas, 19000, Setif, Algeria

[3]University of Bejaia 06000, Bejaia, Algeria
[4] University Bretagne Sud, UMR CNRS 6027, IRDL, Lorient, F-56100, France.

Abstract

The effects of natural aging on low-density polyethylene (LDPE) films exposed to the environmental conditions of Setif (Algeria), known for its continental semi-arid climate, were examined. Over an 18-month natural weathering period, the structural and thermal properties were investigated using various techniques such as UV-Vis and FTIR spectroscopy, X-ray diffraction spectroscopy (XRD) and differential scanning calorimetry (DSC). The films were also subjected to mechanical tensile testing while the rheological properties and the morphological characteristics were examined using, respectively, a parallel-plate rheometer and Atomic Force Microscopy (AFM). The results indicated significant changes in crystallinity and crystallite size, as well as notable modifications in mechanical properties, including tensile strength and elongation at break. The effect of the natural al UV radiation was also reflected by the increase in the complex viscosity, which can be attributed to UV-induced crosslinking reactions and the alterations in surface properties validated by Atomic Force Microscopy (AFM) analysis.

Keywords: Low-density polyethylene, Photooxidation, Natural ageing, Greenhouses, Crystallinity, AFM.

Article History

Received: 22-01-2025
Accepted: 19-05-2025
Published: 30-09-2025

1 Introduction

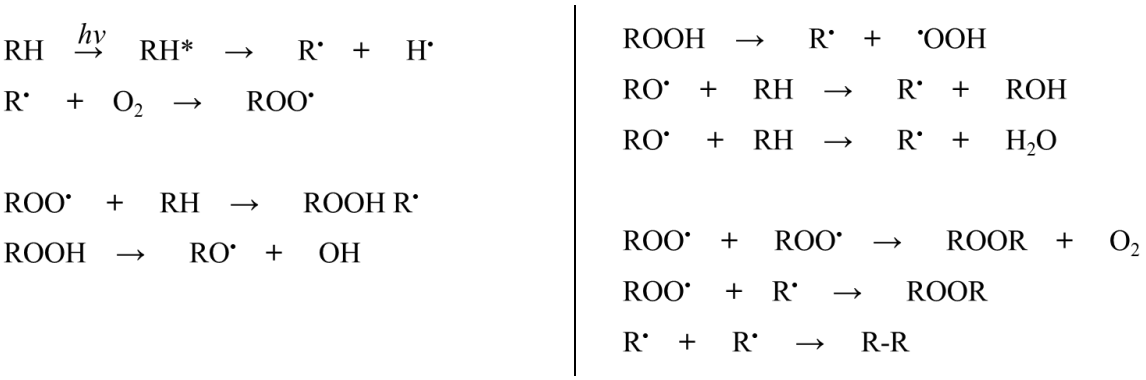
Low-density polyethylene (LDPE) is widely recognized as a superior material for agricultural uses like greenhouses and mulching due to its excellent mechanical properties, transparency, durability, and

* Corresponding author
Email (souad.djellali@univ-setif.dz)

cost-effectiveness. Its light transmission and thermal insulation capabilities support plant growth, while customizable films improve photosynthesis through uniform light diffusion [1,2].

However, despite its advantages, LDPE has faced criticism for its environmental impact. As a non-biodegradable polymer, its extensive use in agriculture contributes to plastic pollution. Discarded LDPE films often persist in the environment, breaking down into microplastics that contaminate soil and water [3,4]. Many authors reported that while certain microorganisms have been identified to metabolize polyethylene fragments, their efficiency is insufficient to address the volume of waste generated [5–7]. Due to LDPE's resistance to natural degradation, scientists are innovating to improve its sustainability by incorporating pro-degradant additives and using controlled environmental conditions to accelerate its breakdown [8–10]. However, these methods are not yet widely implemented in large-scale agricultural practices.

The natural degradation of LDPE is a complex and protracted process. LDPE's chemical structure, characterized by long hydrocarbon chains and low crystallinity, makes it resistant to biodegradation and photo-oxidation [11] . In natural environments, the degradation process primarily involves UV radiation, heat, and oxygen, leading to oxidative breakdown and the formation of smaller molecular fragments [12] (**Scheme 1**). This process, known as photo-oxidation, generates carbonyl and hydroxyl groups, which further weaken the polymer matrix over time[13].



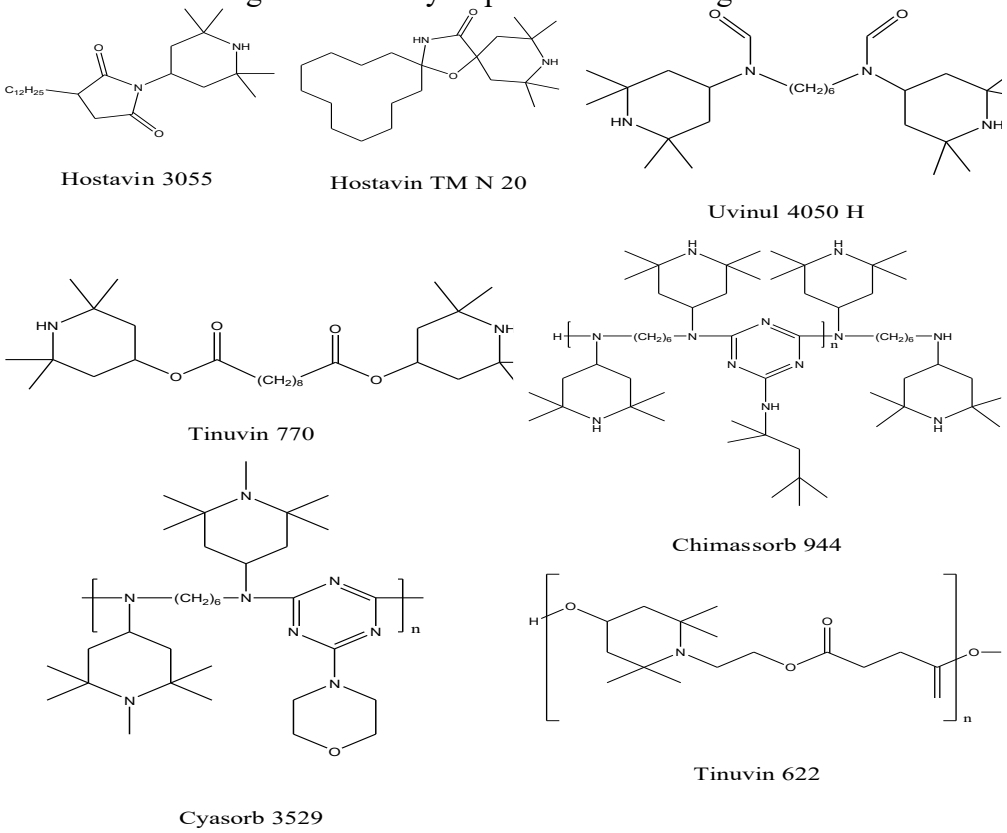
Scheme 1: Mechanism of photo-oxidative degradation [14].

To address the durability challenges posed by prolonged exposure to sunlight and heat, hindered amine light stabilizers (HALS) (Scheme 2) are widely used in LDPE films for agricultural applications. HALS are highly effective in preventing photodegradation, a common issue in greenhouse and mulching films exposed to harsh environmental conditions [15]. These stabilizers function by scavenging free radicals generated during UV exposure, thereby inhibiting the chain reactions that lead to polymer breakdown (Scheme 3). As a result, HALS-treated LDPE films exhibit improved longevity, retaining their mechanical properties and optical clarity over extended periods [16].

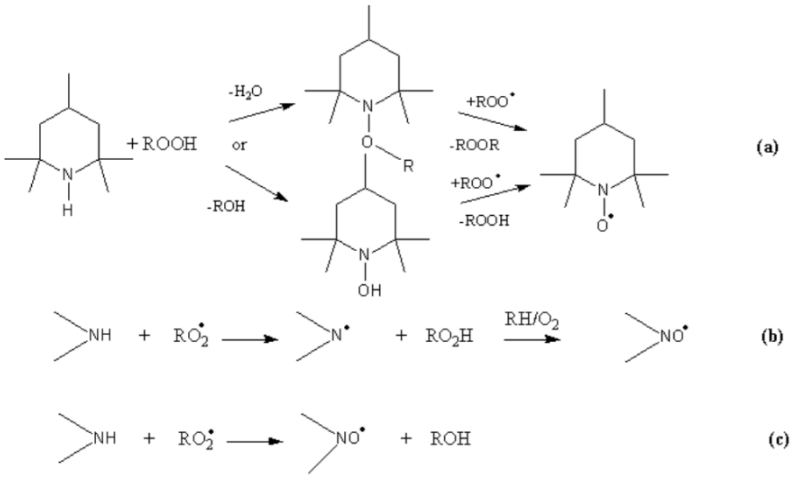
Nonetheless, despite the environmental challenges posed by LDPE waste, its role in revolutionizing the agriculture field in the broader Mediterranean region, including Algeria, is significant [17]. Indeed, by utilizing LDPE films, greenhouses enable farmers to optimize conditions for plant growth, extend growing seasons, and increase crop diversity. These benefits are particularly valuable in Algeria, where agricultural strategies aim to increase productivity and where climatic conditions often limit traditional farming practices. LDPE-based greenhouses have been instrumental in improving food security, promoting high-value crops such as tomatoes, peppers, and cucumbers [18]. Additionally, LDPE mulching enhances soil moisture retention, suppresses weed growth, and regulates soil temperature, crucial for water efficiency in drought-prone areas. These practices address challenges like extreme temperatures, limited water availability, and soil degradation, promoting sustainable agriculture. However, the sustainable management, including recycling and developing biodegradable alternatives, is vital to balance productivity with ecological responsibility.

In this study the efficiency of commercialized LDPE films stabilized with UV-stabilizers (HALS) was evaluated under environmental conditions of Setif (Algeria), known for its continental semi-arid climate. The changes in LDPE films, exposed for 18 months to natural weathering, were examined by

spectroscopic techniques (UV-Vis, FTIR XRD), thermal analysis (DSC), mechanical tensile test, rheological and morphological analysis (AFM). This study underscores the importance of understanding how environmental factors influence polymer degradation over time, which is essential for optimizing material selection and enhancing the durability of products used in agricultural and commercial settings.



Scheme 2: Chemical structures of some hindred amine light stabilizers (HALS) [19].



Scheme 3: Possible mechanisms of HALS action (a): with hydroxyls or alkyloxyamine; (b) and (c) with peroxy radical [20].

2 Materials And Methods

2.1 LDPE films aging

LDPE films (density of 0.92 and MFI of 0.33g/10min) were manufactured through an industrial extrusion blow-molding process and stabilized using Ampacet additives (hindered amine light stabilisers) before undergoing natural weathering in Setif (Algeria) for 18 months. The province of Setif (latitude 36°09′ N, longitude 5°26′ E) is located at approximately 1,100 meters above sea level and experiences a continental semi-arid climate, characterized by scorching summers and freezing winters which create a demanding environment for testing.
The exposure was performed on rectangular samples of the stabilized LDPE films following the ASTM D1435 standard, with a 45° inclination facing south. Samples were periodically collected every three months to assess the effects of natural aging over the testing period.

2.2 UV-Vis and FTIR spectroscopy

The unaged and aged LDPE films' surface were analyzed using the atomic force microscopy (AFM) method. The surfaces topology and roughness were assessed by capturing AFM images with an MFP-3D AFM (Oxford Instruments Asylum Research) in contact mode, employing a silicon cantilever with a lateral resolution of approximately 0.1 nm. The Root Mean Square (RMS) roughness values were computed from the height data in the AFM images. The samples were carefully stored were maintained in a dry environment to prevent moisture absorption.[1]

2.3 UV-Vis and FTIR spectroscopy

XRD characterization was peformed on an X'Pert PRO PANalytical diffractometer using an X-rays beam (CuKα) with a wavelength (λ) of 1.542 Å. The areas under the crystalline and amorphous portions were used to calculate the degree of crystallinity (xc) using the following equation:

$$X_C = \frac{I_c}{I_c + I_a} \qquad (1)$$

where Ia and Ic are the integrated intensity corresponding to the amorphous and crystalline phases, respectively.

The distance between parallel planes of atoms in a crystal lattice, the interplanar distance (d_{hkl}) is calculated using Bragg's law, expressed as:

$$d_{hkl} = \frac{\lambda}{2sin(\theta_{hkl})} \qquad (2)$$

where λ is the wavelength of the X-rays, and θhkl the is the angle of diffraction associated with the lattice planes (hkl).

2.4 Differential scaning calorimetry analysis

Differential Scanning Calorimetry (DSC) measurements for LDPE films were performed using a using a Perkin-Elmer Pyris 1 DSC machine, equipped with Pyris V 8.0 software. The

procedure involved three consecutive heating and cooling cycles under a nitrogen atmosphere, with a ramp rate of 10°C/min across a temperature range from 25°C to 160 °C.

2.5 Tensile test

Tensile properties were measured at room temperature using an MTS Synergie RT1000 testing apparatus at 1 mm/min cross-head speed. Dog-bone shaped specimens, cut from 1 mm thick plates, according to ISO 527-2 standards. Young's modulus, tensile strength, and elongation at break were calculated from force vs. elongation traces. Each sample was measured at least six times to obtain an average value.

2.6 Rheological measurements

Dynamic rheological measurements were conducted using an ARES parallel-plate rheometer with 25 mm plates and a 1 mm gap. A 5% strain ensured linear viscoelasticity, with frequency sweeps from 0.1 to 100 rad/s at 170ºC under nitrogen to prevent degradation. Samples were preconditioned for 3 minutes and vacuum-dried before testing. Data, averaged over three reproducible measurements, were analyzed using TA Orchestrator software to determine complex viscosity (η*). A good reproducibility was obtained for all samples' curves.

2.7 Morphological study using AFM

The unaged and aged LDPE films' surface were analyzed using the atomic force microscopy (AFM) method. The surfaces topology and roughness were assessed by capturing AFM images with an MFP-3D AFM (Oxford Instruments Asylum Research) in contact mode, employing a silicon cantilever with a lateral resolution of approximately 0.1 nm. The Root Mean Square (RMS) roughness values were computed from the height data in the AFM images. The samples were carefully stored were maintained in a dry environment to prevent moisture absorption.

3 Results and discussion

3.1 UV-Vis spectroscopy analysis

Figure 1 shows the UV-Vis absorption spectra of LDPE films containing the photostabilizer, recorded at different exposure times to natural ageing. LDPE typically exhibits a flat and featureless absorption profile in the UV and visible regions due to the lack of chromophores or conjugated systems [21,22]. However, in this study, three absorption bands are observed between 220 nm to 350 nm due to the presence of UV-stabilizer additives. HALS, which are included to enhance UV resistance, act by scavenging free radicals generated during photo-oxidation, preventing the degradation of the material.

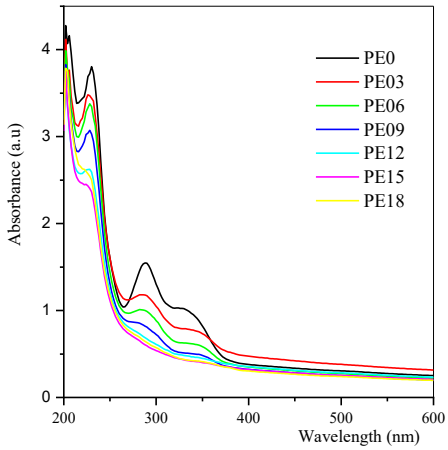


Figure 1: UV-Vis absorption spectra of LDPE films at varying exposure times.

Over an exposure period ranging from 0 to 18 months, a decrease in the intensity of these absorption bands was noted, suggesting the loss of stabilizers due to environmental exposure. This loss, caused by factors such as chemical reactions or physical leaching, ultimately reduced the film's efficacy in providing UV protection. Interestingly, there's a slight increase in absorption at 230 nm, attributed to the $\pi \rightarrow \pi^*$ transitions of C=C (carbon-carbon double bonds) and C=O (carbon-oxygen double bonds). This suggests the formation of new chemical bonds as a result of prolonged exposure

3.2 FTIR spectroscopy analysis

The FTIR spectra of virgin low-density polyethylene (LDPE) serve as a reference for its chemical composition and structure, characterized by prominent peaks attributed to C-H vibrations of methylene groups in the 2800-3000 cm^{-1}, 1460-1470 cm^{-1} and 720-730 cm^{-1} regions. The fingerprint region (600-1500 cm^{-1}) shows typical hydrocarbon chain vibrations. Notably, virgin LDPE lacks significant peaks in the 1700-1800 cm^{-1} (carbonyl groups) and 3200-3600 cm^{-1} (hydroxyl groups) regions, indicating the absence of oxidative degradation and hydrolysis[23].

The effects of the exposure to the natural weathering on the chemical structures of LDPE films are reflected by the noticeable changes in the corresponding spectra as revealed in figures 2-b to 2-g. The emergence of peaks in 1700-1800 cm^{-1} and in the 1100-1300 cm^{-1} regions, indicative of the formation of carbonyl groups and C-O-C bonds, highlights the alterations in the polymer structure such as chain scission or crosslinking; however, the increasing intensities of C-O-C bonds' peaks go to favor of the crosslinking suggestion.

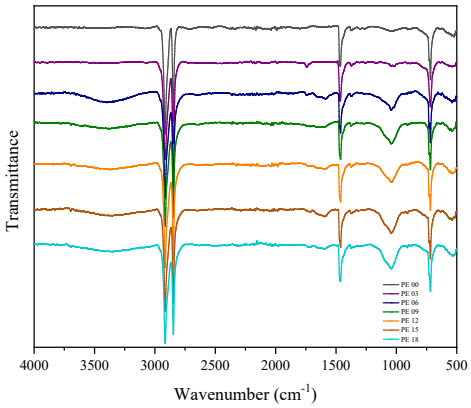


Figure 2 : FTIR spectra of LDPE films subjected to different exposure intervals.

Additionally, the increased absorbance in the 3200-3600 cm^{-1} range suggests the presence of hydroxyl groups, suggesting hydrolysis or the formation of alcohols and acids due to the oxidative degradation [24]. These findings collectively demonstrate the susceptibility of LDPE films to environmental stressors, impacting their mechanical and thermal properties.

3.3 XRD Characterization

Characterization via X-ray diffraction is widely used to assess the structural changes occuring in materials at the atomic level. The results from X-ray diffraction analysis of unaged and aged polyethylene films are illustrated in Figure 3. The XRD patterns for all samples reveal characteristic peaks of low-density polyethylene associated with specific crystallographic planes, such as (110), (200), and (020) indicating a well-defined crystalline structure [14]. The characteristics of these peaks, namely the peak intensity, their position (2θ) and the interplanar distance (d) together with the crystallinity ratios are gathered in Table 1 and Table 1, respectively.

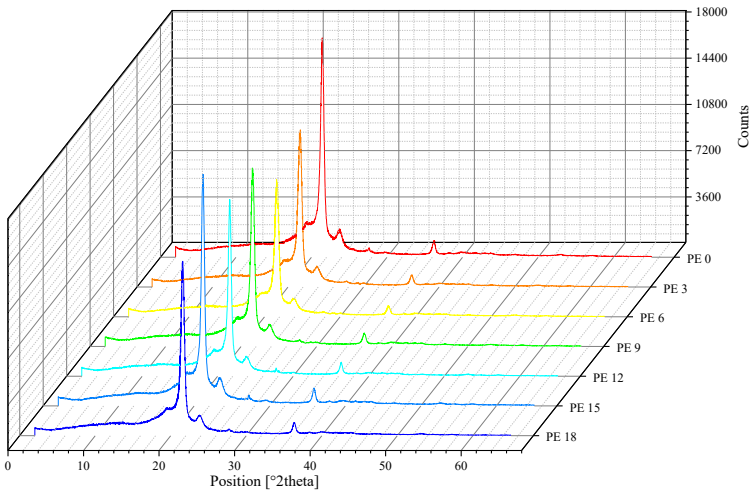


Figure 3 : XRD diffractograms of LDPE films before and after degradation.

Exposure time	Peak intensity	2Theta (°)	d (hkl)	Exposure time	Peak intensity	2Theta (°)	d(hkl)
0	3514.59	21.4626	4.14715	12 months	5864.09	21.56621	4.11723
	265.46	23.67553	3.76430		199.8	23.90429	3.72879
	214.65	36.21402	2.47850		359.47	36.2977	2.47298
3 months	3480.25	21.45608	4.13811	15 months	7965.61	21.12607	4.20200
	383.28	23.85292	3.72745		513.65	23.41726	3.80523
	270.23	36.3294	3.72745		477.89	35.81825	2.50497
6 months	4973.21	21.58833	4.11306	18 months	5693.16	21.55097	4.12010
	327.7	23.73757	3.75460		501.76	23.82395	3.73191
	400.82	36.37557	2.46786		441.49	36.32095	2.47145
9 months	5227.42	21.44762	4.13973				
	633.13	23.9451	3.71330				
	204.34	36.34758	2.47583				

Table 1: XRD parameters for PE samples.

From PE0 to PE18, the crystallinity increases from 36.45% to 49.26%, reflecting a significant structural transformation due to the degradation of amorphous regions, which are more susceptible to environmental factors. *This increase is partly attributed to the replacement of C-H bonds by C=O bonds in the amorphous regions, as evidenced by FTIR results. Secondary crystallization, driven by seasonal temperature variations, also contributes to the rise in crystallinity [25,26]. In the initial phase (PE0–PE6), the moderate increase suggests early-stage degradation, while the intermediate phase (PE6–PE12) shows temporary stabilization. The final phase (PE12–PE18) exhibits a sharper increase, indicating advanced degradation and further growth of existing crystallites or coalescence of smaller crystals. The interchain distances remain unchanged, as evidenced by minimal variation in peak angles, while the lattice strain decreases due to the reorganization and stabilization of the polymer network. These changes indicate a shift towards a more brittle structure with reduced mechanical flexibility over time.

From the above results, the increase in the crystallinity from 36.45% (PE0) to 49.26% (PE18), highlights significant structural changes due to the degradation of the polymer chains and the rearrangement to more reorganized domains, which are more vulnerable to environmental effects. This increase is partially linked to the substitution of C-H bonds with more polar groups such as C=O and O-H bonds, as confirmed by FTIR results. Seasonal temperature variations further drive secondary crystallization, contributing to the rise in crystallinity. During the initial phase (PE0–PE6), a moderate increase reflects early-stage degradation, while the intermediate phase (PE6–PE12) shows temporary stabilization. In the final phase (PE12–PE18), a sharper increase suggests advanced degradation and crystallization of smaller crystals, leading to larger crystallite sizes. Despite this, interchain distances remain unchanged, with minimal variation in peak angles, while decreased lattice strain indicates polymer network reorganization and stabilization. These transformations result in a more brittle structure with reduced mechanical flexibility over time.

	PE0	PE3	PE6	PE9	PE12	PE15	PE18
Crystallinity %	36.45	38.96	42.55	42.84	41.83	46.10	49.26

Table 2: The degree of crystallinity of PE.

3.4 DSC Thermal analysis

The DSC thermograms obtained for unaged and aged LDPEs during heating and cooling cycles are illustrated in figures 4.a and 4.b. The heating cycle analysis of LDPE films subjected to natural aging reveals a small shift of the melting temperature of the initial film from 108.5°C to higher temperatures (110.5°C). While modest, this transition temperature shift reflects aging-induced reorganization of the crystalline domains, as evidenced by corresponding XRD peak

The cooling cycle thermograms further substantiate these findings by displaying a crystallization peak at 97°C, indicating the films' ability to reorganize into crystalline domains upon cooling. This demonstrates that the material retains its structural integrity and capacity for crystallization even after extended exposure. Additionally, the consistent αc relaxation temperature at 61°C across all samples suggests that the amorphous phase of the LDPE remains largely unaffected by natural aging, underscoring the stability of the films' non-crystalline regions.

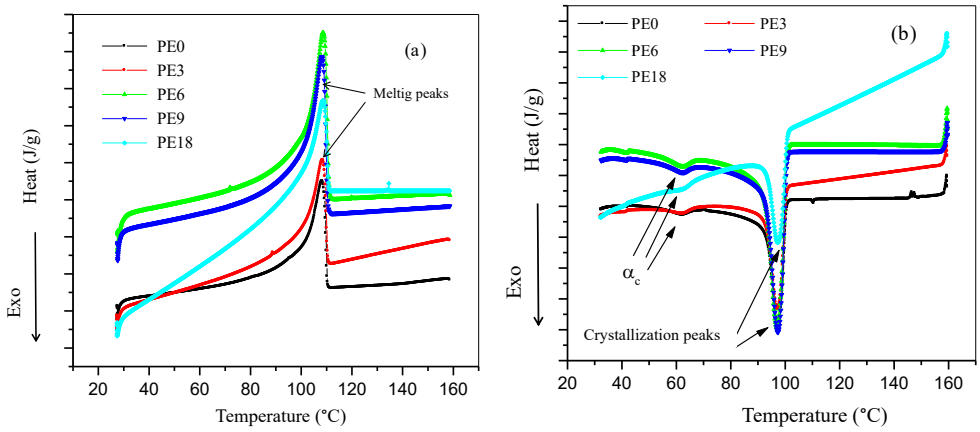


Figure 4: DSC thermograms of LDPE films before and after exposure to natural weathering

3.5 Mecanical tensile test

The low-speed stress-strain test for LDPE films exposed to the various aging periods was very useful to well illustrate the changes induced in terms of the elongation at break, the tensile strength and the elasticity modulus. Figure 5 presents the evolution of three mechanical properties of LDPE films, tensile strength at break, elasticity modulus, and elongation at break, over 18 months of natural weathering.

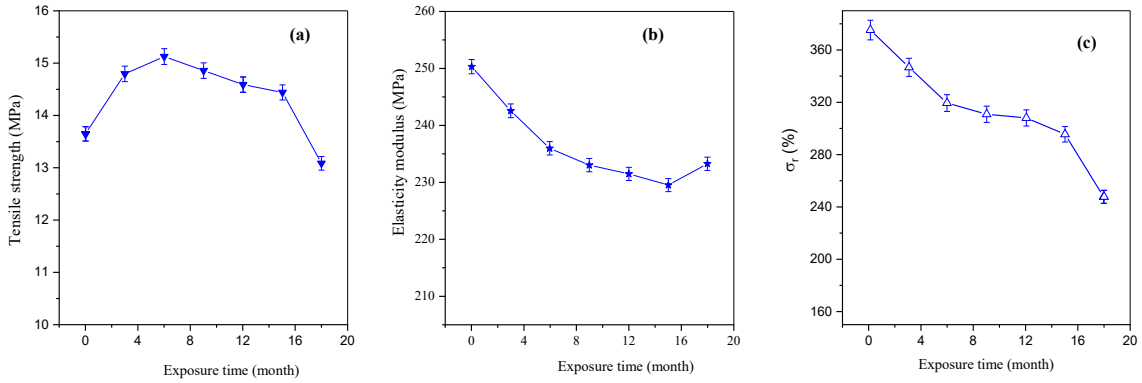


Figure 5: Variations in the tensile mechanical properties of aged films as a function of exposure time: a) Tensile strength at break b) Elasticity modulus c) Elongation at break

The tensile strength at break (Figure 5.a) initially increases within the first 3 months, likely due to UV-induced cross-linking, which temporarily enhances the material's strength, however, between 3 and 12 months, this property stabilizes, indicating a balance between cross-linking and degradation. After 12 months, the tensile strength at break drops, suggesting a degradation processes such as oxidative chain scission and embrittlement. On the other hand, the elasticity modulus (Figure 5.b) and the elongation at break (Figure 5.c) decrease steadily over the 18 months. This trend indicates a progressive loss of stiffness in the LDPE film, as polymer chains break and structural integrity declines due to prolonged environmental exposure, including UV radiation, oxygen, and moisture. These results highlight the progressive deterioration of LDPE films under natural weathering. Cross-linking and chains scission processes initially counteract degradation, enhancing tensile strength temporarily. However, over time, oxidative degradation and chain scission dominate, leading to reduced stiffness, strength, and elongation capacity. This combined effect compromises the mechanical performance and lifespan of LDPE films in outdoor applications.

3.6 Rheological properties of LDPE films before ad after ageing

Results from dynamic rheological study of films exposed to natural ageing for 18 months, determined using a plate-plate rheometer, are depicted in Figures 6 and 7. These figures respectively illustrate the variation in complex viscosity (η*) as a function of shear rate and the change in viscosity of the films over the duration of exposure to natural aging.

The complex viscosity-shear rate curves (Figure 6) exhibit similar shapes for all samples. At low shear rates, the viscosity remains nearly constant across all samples indicative of a shear thinning behaviour [27]. However, at high shear rates, the viscosity significantly decreases until it approaches values near zero. Regarding the viscosity of the films, an increase with exposure time is noticed, as confirmed by Figure 6, which shows a gradual rise in viscosity with increased exposure time, reaching a plateau after more than 9 months of exposure. Figure 7 indicates that the viscosity increases linearly up to 9 months of exposure to natural aging, after which the increase slows down, reaching a plateau at 97 KPa.s.

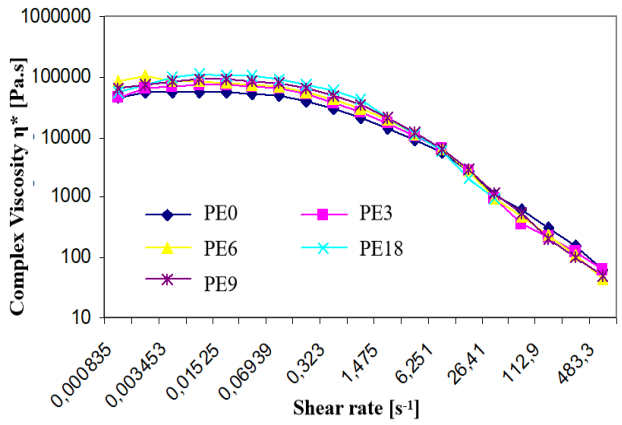


Figure 6: Complex viscosity of LDPE films exposed to natural ageing as a function of shear rate at T = 170 °C

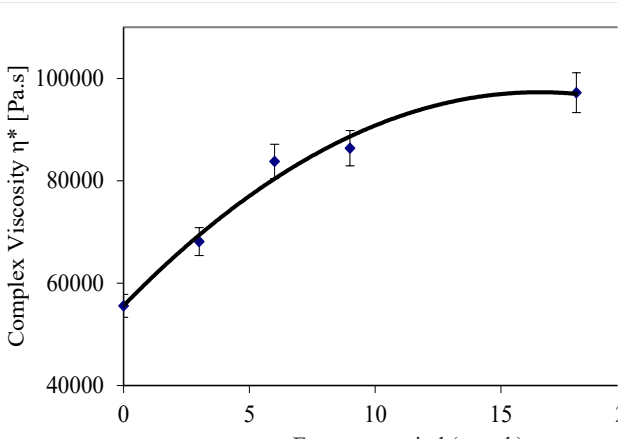


Figure 7: Complex viscosity of LDPE films exposed to natural ageing as a function of exposure time (γ = 0.0039 s^{-1})

3.7 Surface caracterisation (AFM)

The atomic force microscopy (AFM) allows for a comprehensive analysis of films at both micro and nano scales, highlighting the impact of aging on surface properties. The results obtained from this

analysis are illustrated in Figure 8a and 8b for LDPE films before ageing and after 18 months ageing, respectively. Indeed, using contact mode AFM, the observed surface after degradation exhibits rougher and intricate morphology with more frequent undulations, compared to undegraded film, as reported in Table 3.

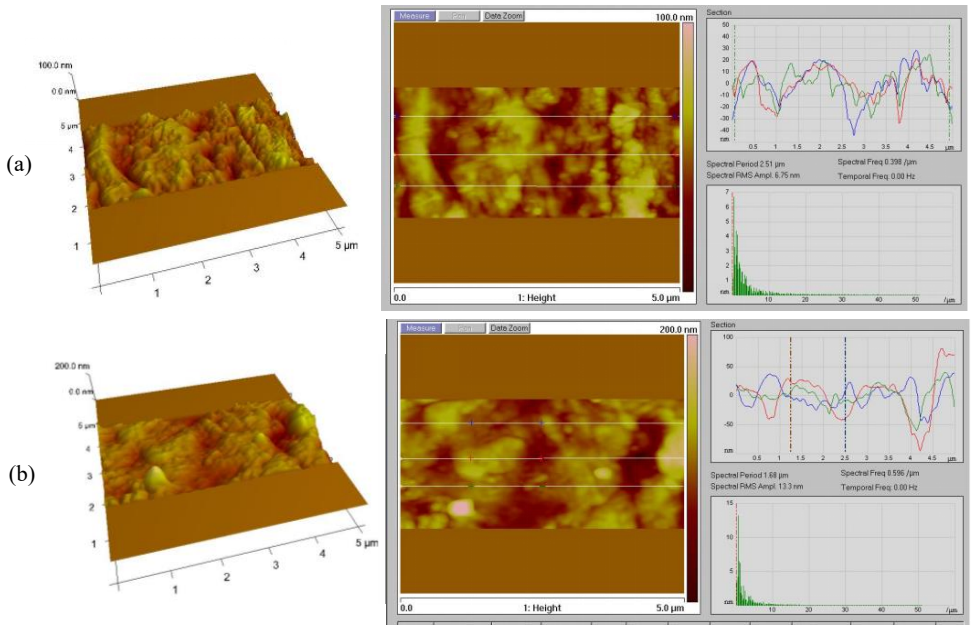


Figure 8 : AFM Images LDPE film

a) Before ageing b) After 18 months ageing

Parameter	Initial LDPE films	Aged LDPE films
Spectral RMS Amplitude	6.75 nm	13.3 nm
Maximum Height Variation	100 nm	200 nm
Spectral Period	2.51 µm	1.68 µm
Surface Features	Broad, widely spaced undulations.	Finer, more frequent undulations.
Dominant Characteristics	Smooth, relatively uniform.	Rougher, intricate morphology.

Table 3: AFM results for LDPE films' surfaces before and after natural aging

4 Conclusion

This study examined the impact of natural ageing on LDPE films subjected to semi-arid environmental conditions in Setif, Algeria, over a period of 18 months. The material performance was assessed using various effective methodologies. The spectroscopic examination employing UV-Vis and FTIR validated the presence of several chemical functionalities (hydroxyls, acids, esters, etc.) resulting from oxidative degradation. Furthermore, the X-ray diffractograms and DSC thermograms indicate a notable tendency of increased crystallinity in LDPE with prolonged exposure time. This structural modification has influenced the mechanical, morphological, and

rheological properties of aged LDPE films in comparison to the unaged films. Consequently, when LDPE films are subjected to heat or UV radiation, they experience oxidation, resulting in the concurrent processes of chain scission and cross-linking. These findings are essential for comprehending the durability and performance of LDPE films in analogous conditions, highlighting its prospective applications in greenhouse coverings and packaging materials.

References

[1] A. Al-Mahdouri, M. Baneshi, H. Gonome, J. Okajima, S. Maruyama, Evaluation of optical properties and thermal performances of different greenhouse covering materials, Solar Energy 96 (2013) 21–32. https://doi.org/10.1016/j.solener.2013.06.029.

[2] S. Ghani, F. Bakochristou, E.M.A.A. ElBialy, S.M.A. Gamaledin, M.M. Rashwan, A.M. Abdelhalim, S.M. Ismail, Design challenges of agricultural greenhouses in hot and arid environments – A review, Engineering in Agriculture, Environment and Food 12 (2019) 48–70. https://doi.org/10.1016/j.eaef.2018.09.004.

[3] H. Jiao, S.S. Ali, M.H.M. Alsharbaty, T. Elsamahy, E. Abdelkarim, M. Schagerl, R. Al-Tohamy, J. Sun, A critical review on plastic waste life cycle assessment and management: Challenges, research gaps, and future perspectives, Ecotoxicology and Environmental Safety 271 (2024) 115942. https://doi.org/10.1016/j.ecoenv.2024.115942.

[4] J.E. Mendoza, D. Tineo, B. Chuquibala-Checan, N. Atalaya-Marin, V.H. Taboada-Mitma, J. Tafur-Culqui, E. Tarrillo, D. Gómez-Fernández, M. Goñas, M.A. Reyes-Reyes, Global perspectives on the biodegradation of LDPE in agricultural systems, Front. Microbiol. 15 (2025) 1510817. https://doi.org/10.3389/fmicb.2024.1510817.

[5] S. Djellali, N. Benmahmoud, T. Sadoun, Biodegradation of low density polyethylene/starch films exposed to soil burial, Ann. Chim. Sci. Mat. 34 (2009) 41–48. https://doi.org/10.3166/acsm.34.41-48.

[6] S. Kumar Sen, S. Raut, Microbial degradation of low density polyethylene (LDPE): A review, Journal of Environmental Chemical Engineering 3 (2015) 462–473. https://doi.org/10.1016/j.jece.2015.01.003.

[7] A.A. Shah, F. Hasan, A. Hameed, S. Ahmed, Biological degradation of plastics: A comprehensive review, Biotechnology Advances 26 (2008) 246–265. https://doi.org/10.1016/j.biotechadv.2007.12.005.

[8] H. Boughrara, S. Djellali, N. Haddaoui, J.-N. Staelens, P. Supiot, U. Maschke, A facile route to improve compatibilization of low density polyethylene/poly (ε-caprolactone) blends, Polymer Degradation and Stability 204 (2022) 110111. https://doi.org/10.1016/j.polymdegradstab.2022.110111.

[9] S. Djellali, N. Haddaoui, T. Sadoun, A. Bergeret, Y. Grohens, Structural, morphological and mechanical characteristics of polyethylene, poly(lactic acid) and poly(ethylene-co-glycidyl methacrylate) blends, Iran Polym J 22 (2013) 245–257. https://doi.org/10.1007/s13726-013-0126-6.

[10] M. Koutny, J. Lemaire, A.-M. Delort, Biodegradation of polyethylene films with prooxidant additives, Chemosphere 64 (2006) 1243–1252. https://doi.org/10.1016/j.chemosphere.2005.12.060.

[11] R.T. Bachmann, S.K. Ong, Characteristics and degradation of carbon low-density polyethylene (LDPE) composites in the environment, in: Char-Based Composites, Elsevier, 2025: pp. 301–341. https://doi.org/10.1016/B978-0-443-15403-4.00013-7.

[12] A. Albertsson, S. Karlsson, The influence of biotic and abiotic environments on the degradation of polyethylene, Progress in Polymer Science 15 (1990) 177–192. https://doi.org/10.1016/0079-6700(90)90027-X.

[13] J.H. Khan, S.H. Hamid, Durability of HALS-stabilized polyethylene film in a greenhouse environment, Polymer Degradation and Stability 48 (1995) 137–142. https://doi.org/10.1016/0141-3910(95)00015-E.

[14] D. Briassoulis, A. Aristopoulou, M. Bonora, I. Verlodt, Degradation Characterisation of Agricultural Low-density Polyethylene Films, Biosystems Engineering 88 (2004) 131–143. https://doi.org/10.1016/j.biosystemseng.2004.02.010.

[15] A. Rebaya, S.I. Belghith, B. Baghdikian, V.M. Leddet, F. Mabrouki, E. Olivier, J. kalthoum Cherif, M.T. Ayadi, Total phenolic, total flavonoid, tannin content, and antioxidant capacity of Halimium halimifolium (Cistaceae), Journal of Applied Pharmaceutical Science 5 (2015) 052–057.

[16] P. Gijsman, Polymer Stabilization, in: Applied Plastics Engineering Handbook, Elsevier, 2017: pp. 395–421. https://doi.org/10.1016/B978-0-323-39040-8.00018-3.

[17] R. Kumar, V.P. Singh, Plasticulture Engineering and Technology, 1st ed., CRC Press, Boca Raton, 2022. https://doi.org/10.1201/9781003273974.
[18] Organisation des Nations Unies pour l'alimentation et l'agriculture, Société internationale de la science horticole, Centre national pour la recherche agricole et la vulgarisation, eds., Good agricultural pratices for greenhouse vegetable crops: principles for mediterranean climate areas, FAO, Rome, 2013.
[19] C.W. Klampfl, M. Himmelsbach, Advances in the determination of hindered amine light stabilizers – A review, Analytica Chimica Acta 933 (2016) 10–22. https://doi.org/10.1016/j.aca.2016.06.001.
[20] P. Gijsman, A review on the mechanism of action and applicability of Hindered Amine Stabilizers, Polymer Degradation and Stability 145 (2017) 2–10. https://doi.org/10.1016/j.polymdegradstab.2017.05.012.
[21] N.A.G. Gomez, S.A. Maruyama, A. Leuteritz, F. Wypych, Composites of polyethylene and layered cobalt hydroxide salts as potential ultraviolet radiation absorbers, Polym. Bull. 77 (2020) 255–273. https://doi.org/10.1007/s00289-019-02742-x.
[22] S.V. Kumar, B. Ghadei, S.K. Chaudhuri, J.B.M. Krishna, D. Das, A. Saha, Chemical transformations and changes in free volume holes in high-energy proton irradiated low-density polyethylene (LDPE), Radiation Physics and Chemistry 77 (2008) 751–756. https://doi.org/10.1016/j.radphyschem.2007.11.002.
[23] H. Lobo, J.V. Bonilla, eds., Handbook of Plastics Analysis, 1st Ed., Boca Raton, CRC Press, 2003. https://doi.org/10.1201/9780203911983.
[24] M. Hamzah, M. Khenfouch, A. Rjeb, S. Sayouri, D.S. Houssaini, M. Darhouri, V. Srinivasu, Surface chemistry changes and microstructure evaluation of low density nanocluster polyethylene under natural weathering: A spectroscopic investigation, J. Phys.: Conf. Ser. 984 (2018) 012010. https://doi.org/10.1088/1742-6596/984/1/012010.
[25] K. Aljoumaa, M. Abboudi, Physical ageing of polyethylene terephthalate under natural sunlight: correlation study between crystallinity and mechanical properties, Appl. Phys. A 122 (2016) 6. https://doi.org/10.1007/s00339-015-9518-0.
[26] N.C. Billingham, P. Prentice, T.J. Walker, Some effects of morphology on oxidation and stabilization of polyolefins, J. Polym. Sci., C Polym. Symp. 57 (1976) 287–297. https://doi.org/10.1002/polc.5070570134.
[27] S. Djellali, T. Sadoun, N. Haddaoui, A. Bergeret, Viscosity and viscoelasticity measurements of low density polyethylene/poly(lactic acid) blends, Polym. Bull. 72 (2015) 1177–1195. https://doi.org/10.1007/s00289-015-1331-6.